International Journal of Advanced Research in Engineering Technology & Science
ISSN: 2349-2819
Email: editor@ijarets.org Volume-4, Issue-3 March- 2017 www.ijarets.org

A STUDY ON THE MATHEMATICAL MODELING & SIMULATION OF LARGE AND SMALL SCALE STRUCTURES IN STAR FORMATION

M. T. Kolhe

Assistant professor (Department of Mathematics)

Arts,Commerce and Science College Arvi Di-Wardha Maharashtra, India

Abstract

Stars are known to assume a key part in numerous cosmological cycles going from the advancement of the early universe to world development and the formation of planets.. Subsequently, understanding star formation turns into an essential device in getting the universe in general. Numerous properties encompassing star formation can be gathered by studying molecular clouds. Molecular clouds are a profoundly dense interstellar clouds comprised of dominatingly molecular hydrogen.

Bunches inside the cloud joined with adequate gravity give the early phases of star formation. From the get-go in the heavenly advancement timeline, prestellar cores form as a hydrostatic starless area. As the core accumulates mass from the encompassing cloud, the core's self-gravity starts to rule the inward strain causing a breakdown which prompts the formation of a protostar and a protostellar core. Magnetic fields assume a huge part in the formation and dependability of the core. Understanding the magnetic properties of pre and protostellar cores can prompt seeing a portion of the heavenly properties, for example, the compression systems overseeing the breakdown.

Keywords:

Star, protostellar, cores, magnetic

1.Introduction

The magnetic field administering protostellar cores assumes a significant part in star formation. The gas dynamics are affected by the magnetic field, which manages the gravity and can direct the rate of formation [5, 6]. Polarimetry estimations give the best instrument to studying and inducing the magnetic properties.

Construing magnetic field in protostellar cores can be trying because of the restricted accessibility of high resolution polarization maps. Albeit observationally estimated polarization guides of have been inadequate and challenging to drop by, there are still some that have been made accessible lately [7,8]. Given these impediments, hypothetical models are normally utilized in deciphering these estimations and inducing the particular noticeable properties.

The developmental properties administering protostellar cores can be modeled through magnetohydrodynamic (MHD) simulation. Because of the light ionization of the clouds [9], mathematical MHD simulations should be non-ideal to represent the magnetic field not being completely coupled to the plasma. These simulation yields form the reason for a model that can be incorporated with noticed polarimetry data to register manufactured polarization maps. These manufactured guides are utilized to deduce the magnetic field at a given direction that is integrated along the spectator's view.

By mathematically tackling the resistive MHD equations over a nested grid, a progression of protostellar models can be built at different length scales, settling increasingly small areas. For each model result, the radiative exchange code POLARIS can be utilized to reproduce an individual polarization map at a given length scale. The MHD simulations are utilized to create high resolution models inside a simulation shape having side lengths as little as $\approx 90 - 180$ au. These length scales can be more modest than a large part of the noticed polarimetry data currently accessible and empower forecasts for future higher resolution perceptions.

2. Small Scale Structure – Prestellar cores: Non-Ideal Magnetohydrodynamic Simulation

To reenact the dense, star-forming core of molecular clouds, non-ideal magnetohydrodynamic simulations are utilized as the reason for the model. This is a direct augmentation to the model talked about in the past part. In these dense locales, the clouds are daintily ionized [9] and due to this the magnetic field can't be coupled to the plasma thus the motion frozen property is as of now not legitimate.

It is at this stage that the plasma should be treated in a non-ideal MHD design to represent neutrals, particles, electrons and other charged material. The simulations were performed by Machida et al. [10] utilizing their three dimensional nested MHD code that tackles the resistive MHD equations including self-gravity:

1) $$\frac{\partial \rho}{\partial t} + \nabla \cdot (\rho \mathbf{v}) = 0$$

2) $$\rho \frac{\partial \mathbf{v}}{\partial t} + \rho (\mathbf{v} \cdot \nabla) \mathbf{v} = -\nabla p + \mathbf{j} \times \mathbf{B} - \rho \nabla \Phi$$

3) $$\frac{\partial \mathbf{B}}{\partial t} = \nabla \times (\mathbf{v} \times \mathbf{B}) + \eta \nabla^2 \mathbf{B}$$

4) $$\nabla^2 \Phi = 4\pi G \rho$$

for the density ρ, the velocity v and the magnetic field B. Here, Φ is the gravitational potential, j is the electric current density, p is the strain, η is the resistivity and G is the gravitational constant.

2.1 Initial State

As an underlying state, the core embraces a Bonnor-Ebert density profile with a focal density of 6 × 105 cm−3 and isothermal temperature T = 10 K. The underlying core mass and sweep are taken to be Mcl = 2M and Rcl = 1.2 × 104 au, individually. The simulation additionally improves the cloud density by a factor f = 1.68 to advance the compression.

For the underlying core, a uniform magnetic field of B0 = 3.2 × 10−5 G is taken with an unbending rotation of Ω0 = 1.3 × 10−13 s −1 where the rotation axis is corresponding to the magnetic field. Also, the standardized mass-to-motion proportion in the underlying state is taken to be μ0 = 2 which is standardized to the basic worth 1/(2πG1/2). At long last, the proportion of warm and rotational energy to gravitational energy are α0 = 0.42 and β = 0.024, separately.

2.2 Ohmic Dissipation & Sink Treatment

The Ohmic dissipation is modeled by the successful resistivity [11] in the enlistment equation 3. The resistivity η is embraced from Nakano et al. [12] and is quantitatively assessed to being a function of the number density and the temperature:

.5) $$\eta = \frac{740}{\chi_e}\sqrt{\frac{T}{10\mathrm{K}}}\left[1 - \tanh\left(\frac{n}{10^{15}\mathrm{cm}^{-3}}\right)\right] \ \mathrm{cm}^2\mathrm{s}^{-1}$$

for the ionization degree of the gas

$$\chi_e = 5.7 \times 10^{-4}\left(\frac{n}{\mathrm{cm}^{-3}}\right)^{-1}$$

where T is illustrative of the gas temperature and n is the number density. At last, the MHD simulation embraces a sink at the focal point of the simulation grid to accelerate the estimation. Taking the 'sink sweep's rsink = 2 au, the area r < rsink eliminates gas having number density n > 1012 cm−3 from the simulation grid and adds it to the protostar as gravity for each timestep. For n < 1012 cm−3 the equation of state is taken to address an isothermal ideal gas.

2.3 Mathematical Methods

To successfully model the administering transformative properties of the core, the resistive MHD solutions of Machida et al. are utilized. Their mathematical code tackles the three dimensional resistive MHD equations on a nested grid involving a Monotonic Upstream-centered Scheme for Conservation Laws (MUSCL) to the moderate form of the MHD equations:

6)
$$\frac{\partial \mathbf{U}}{\partial t} + \nabla \cdot F(\mathbf{U}) = 0$$

where U addresses the vector of saved variables and F(U) addresses the motion of rationed variables.

Figure 1 gives a schematic portrayal of a nested grid in two aspects. Forcing this calculation refines the cross section toward the focal point of the area and keeps the lattice coarse nearer to the limits. The mathematical scheme increases the simulation on the nested grid to three aspects and gatherings the results into levels illustrative of a given scale inside the simulation block. Each level is comprised of 64 cells across each aspect where the amounts of interest are assessed at the focal point of every cell situated at:

$$x_i^{(l)} = 2^{-l+1}\left(i + \frac{1}{2}\right)h \qquad y_j^{(l)} = 2^{-l+1}\left(j + \frac{1}{2}\right)h \qquad z_k^{(l)} = 2^{-l+1}\left(k + \frac{1}{2}\right)h$$

for a stage size h that is divided at each level and the superscript l being a given simulation level. Each positional list I, j, k is limited as −N/2 ≤ I, j, k ≤ N/2 − 1. The block has volume V = L 3 = (Nh) 3 and the simulation runs for 13 levels absolute (just levels 5 - 13† are considered since before stages don't present critical systematic advancement of the protostellar core).

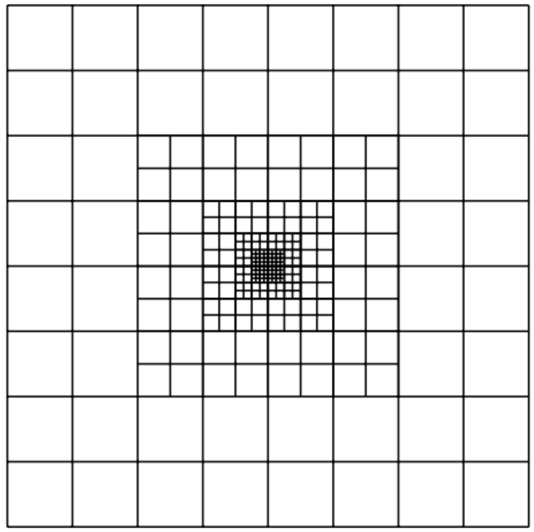

Figure 1: Exemplary geometry of a nested grid demonstrated for a total of 5 levels of refinement

2.4 MHD Simulation Output

The MHD simulations approach t ≈ 89547 years, which compares to a mass of M ≈ 0.3M in the core's advancement. The simulation yields are demonstrated through figures at each level inside the nested grid. Subsequently, each figure shows 8 or 9 distinct plots from level 5 up to and including levels 12 and 13. The essential examination of the simulations reads up the core's structure for three phases in the transformative cycle for when M = 0.01M ; M = 0.2M and M = 0.28M.

These results will be reached out to mimicking engineered polarization maps at all levels in the nested grid. This system will take into consideration high resolution figures of the limited scale areas inside protostellar cores. Moreover, to all the more likely imagine the core's dynamics, figure 30 demonstrates the time development of the plasma surge as the core has advanced to M = 0.15M, M = 0.25M and M = 0.30. These plots are taken at level 7 in the nested grid as a midplane cut at the 32nd cell and are displayed in the x − z, y − z and x − y planes.

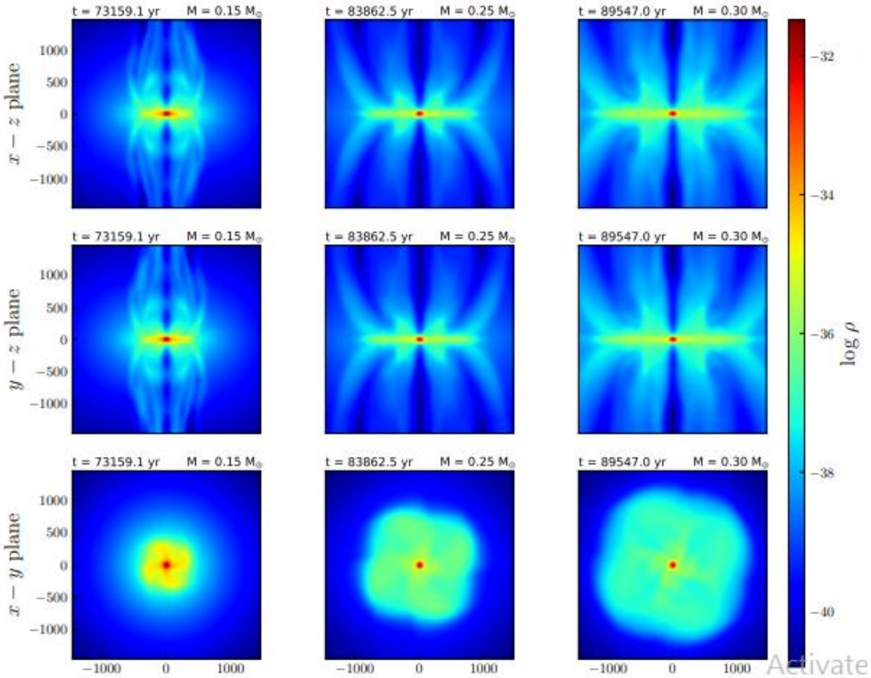

Figure 2: Density (g/cm3) given to demonstrate the time evolution of the outflow as the core evolves. Figure is given for the level 7 stage in the simulation grid. Axis units are given in au.

Magnetic Field:

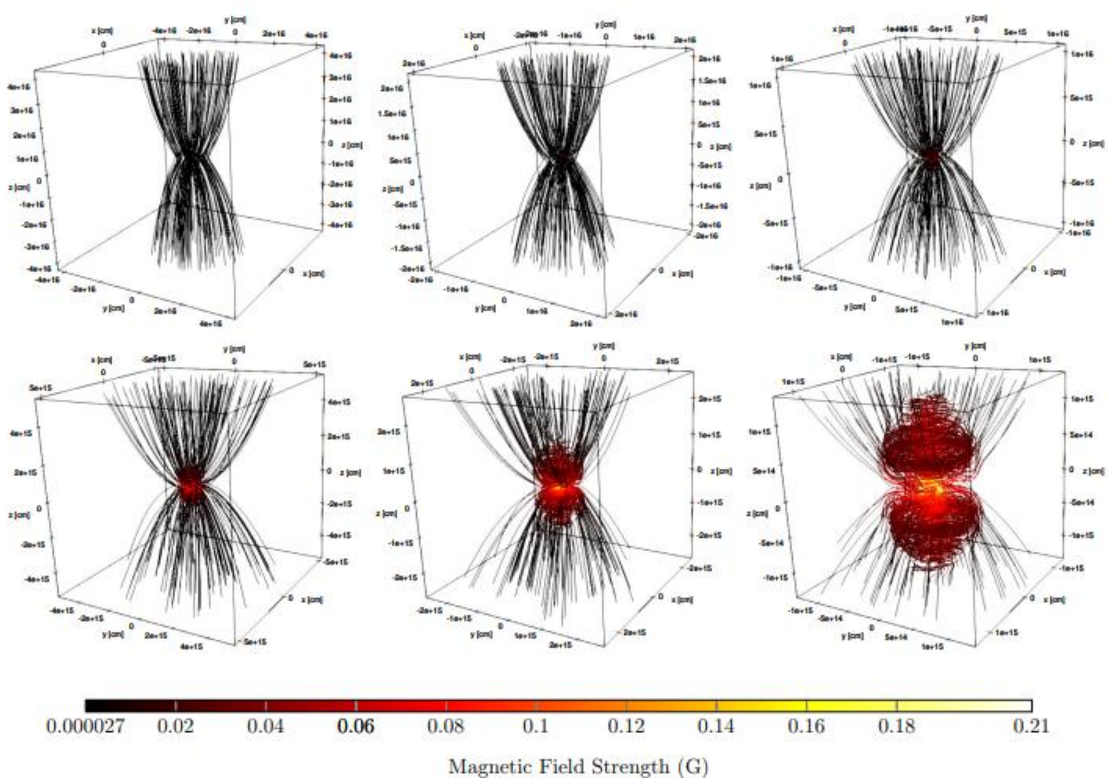

Velocity Field:

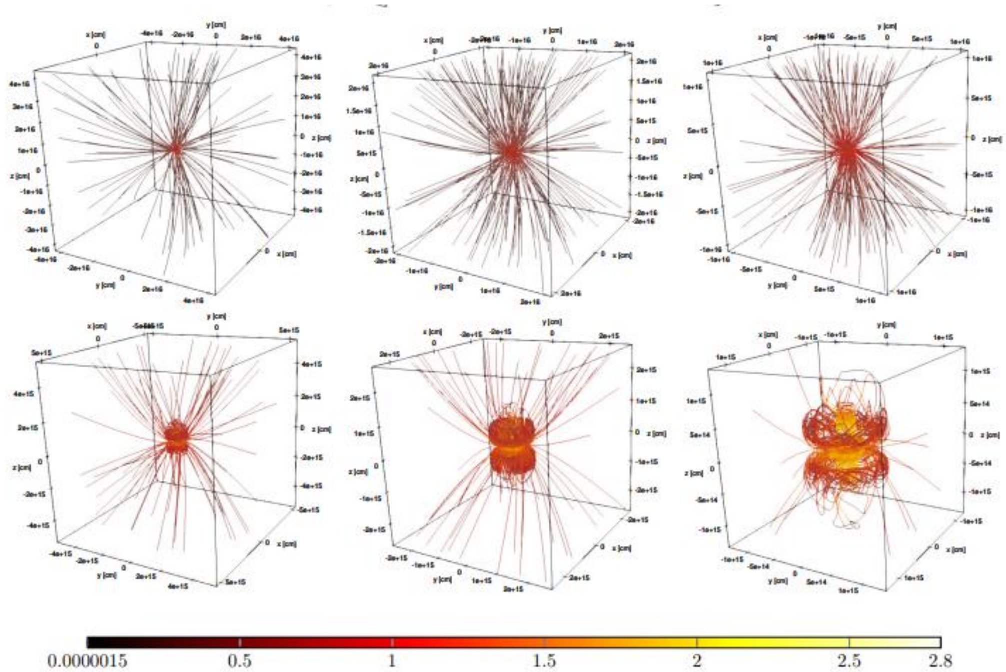

Velocity Field Magnitude (cm/s)

3. Large Scale Structure – Prestellar cores : Non-Ideal Magnetohydrodynamic Simulation

Numerous properties administering prestellar cores are connected to the actual properties of the incorporating molecular cloud preceding dynamical breakdown. The stringing magnetic field is a significant deterministic factor in the soundness of the cloud [3, 4].

The cloud is supposed to be magnetically supercritical in the event that the constriction component is gravitationally overwhelmed, hauling field lines internal with the direction of withdrawal. This situation happens quickly on the dynamical time scale. Besides, the core is in a magnetically subcritical state in the event that the compression instrument is magnetically determined because of the semi static advancement from the float of nonpartisan particles through ambipolar diffusion. The subcritical situation happens on significantly longer time scales.

The float of nonpartisan particles toward the focal point of the cloud gradually expands the mass to transition proportion M/Φ [4]. A cloud that is magnetically subcritical has a mass to motion proportion more modest than some characterized basic proportion (M/Φ)crit which is given for instances of impeccably adjusted gravitational and magnetic commitments to withdrawal.

When M/Φ > (M/Φ)crit the cloud has now progressed to a supercritical state which sets off the beginning of dynamical breakdown. A cloud that is at first in the supercritical state goes through dynamical breakdown sooner except if there is inward warm and violent tension for help [4]. This inspires further examination of the magnetic properties in these prestellar cores.

A gauge of the magnetic field morphology and possibly even magnetic field strength can be utilized to decide the magnetic state of the core regarding its solidness. Considering that polarimetry can be utilized to deduce the magnetic field morphology, it can't be utilized to directly appraise magnetic field strength. This is because of there being numerous vulnerabilities in the properties of the residue grains and the particular proficiency in their arrangement instruments.

Direct estimation is conceivable through Zeeman impact yet has demonstrated to be troublesome because of estimation awareness and resolution. With the developing example of polarization maps accessible, it is vital to foster vigorous techniques that can surmise the magnetic properties and mass-to-motion proportions from data. A typical strategy to model hourglass structures has been to fit a two dimensional single plane model to polarization sections.

3.1 Mathematical Model

The model accepts a prestellar core is strung with a foundation magnetic field in the z−direction. This foundation field will be misshaped inside the core.

Allow B0 to signify the foundation field given as:

$$B = B_c + B_o$$

where Bc is the nearby magnetic field generated inside the core. The model accepts that the magnetic field is axisymmetric about the ϕ−direction and the magnetic field is taken as B ≡ B(r, z).

The supposition that depends on the reason that the model records for the core for a huge scope and that the bending and anomalies in Bϕ become basic just at the focal point of the core on a scale a lot more modest than that of the actual core.

The model's magnetic field function is gotten directly from Maxwell's equations and yields an unequivocal insightful articulation for the magnetic field parts along the r− and z−directions for a current density that is ordinarily appropriated along the vertical.

This gives a magnetic vector possible function as:

$$A(r,z)=\sum_{m=1}^{\infty}k_m J_1(\sqrt{\lambda_m}r)\left[\operatorname{erfc}\left(\frac{\sqrt{\lambda_m}h}{2}+\frac{z}{h}\right)e^{z\sqrt{\lambda_m}}+\operatorname{erfc}\left(\frac{\sqrt{\lambda_m}h}{2}-\frac{z}{h}\right)e^{-z\sqrt{\lambda_m}}\right]$$

for the coefficients:

$$k_m=\frac{2h\pi^{3/2}e^{h^2\lambda_m/4}}{cR^2\sqrt{\lambda_m}\left[J_2(\sqrt{\lambda_m}R)\right]^2}\int_0^R f(\xi)J_1(\sqrt{\lambda_m}\xi)\xi d\xi$$

The magnetic field can explicitly be found using the relation B = ∇ × A which yields the expressions:

$$B_r(r,z)=\sum_{m=1}^{\infty}k_m\sqrt{\lambda_m}J_1(\sqrt{\lambda_m}r)\left[\operatorname{erfc}\left(\frac{\sqrt{\lambda_m}h}{2}-\frac{z}{h}\right)e^{-z\sqrt{\lambda_m}}-\operatorname{erfc}\left(\frac{\sqrt{\lambda_m}h}{2}+\frac{z}{h}\right)e^{z\sqrt{\lambda_m}}\right]$$

$$B_z(r,z)=\sum_{m=1}^{\infty}k_m\sqrt{\lambda_m}J_0(\sqrt{\lambda_m}r)\left[\operatorname{erfc}\left(\frac{\sqrt{\lambda_m}h}{2}+\frac{z}{h}\right)e^{z\sqrt{\lambda_m}}+\operatorname{erfc}\left(\frac{\sqrt{\lambda_m}h}{2}-\frac{z}{h}\right)e^{-z\sqrt{\lambda_m}}\right]+B_0$$

where km, h, R and B0 are taken as free parameters.

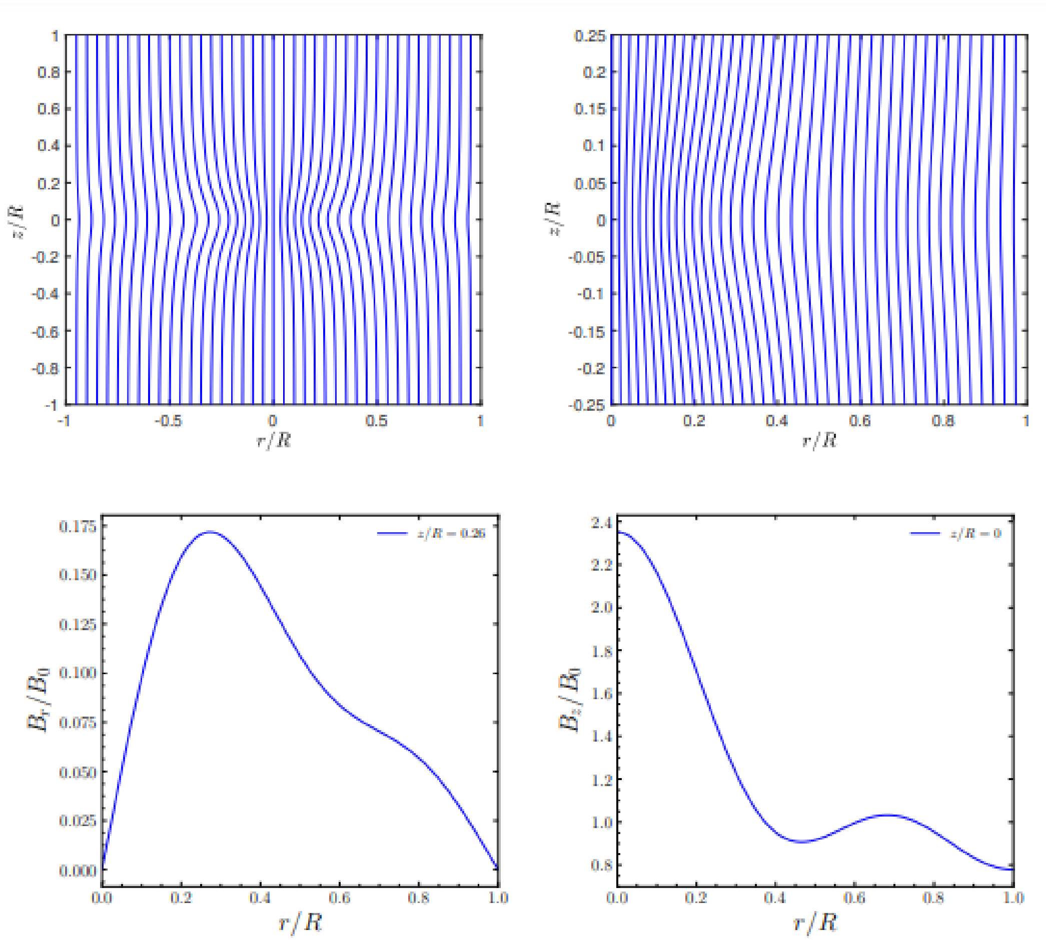

Figure 4: Magnetic field lines (top) and normalized field strength (bottom) using the parameters

3.2 Parameters & Reformulation

It serves worth to talk about the fitting boundaries in the model, basically the foundation field B0. In Basu and Ewertowski (2013) [13], they recommend that the foundation field ought to be independant to the fit. Estimating magnetic field directly is extremely challenging and in this manner more so than not, one goes to indirect strategies to gather the magnetic field. Understanding what B0 means for the hourglass example can give knowledge regarding what the B0 ought to be by and by. For show purposes, the Basu, Ewertowski model boundaries will be utilized and the foundation field will be fluctuated.

Taking a gander at the accompanying figures show that as the foundation field expands, the hourglass design is veiled and overwhelmed by B0.

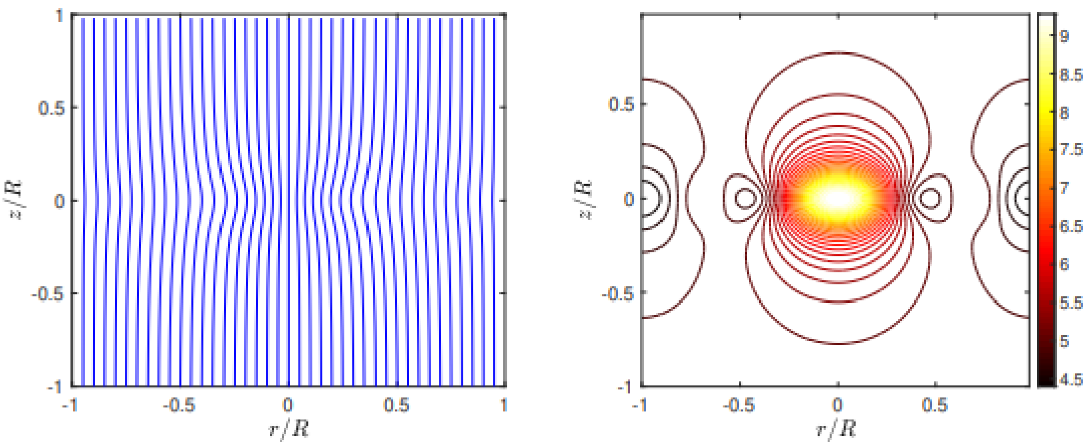

Figure 5: Background field $B = 1.5B_0$. **Left:** Magnetic field lines. **Right:** Contours of the total field strength.

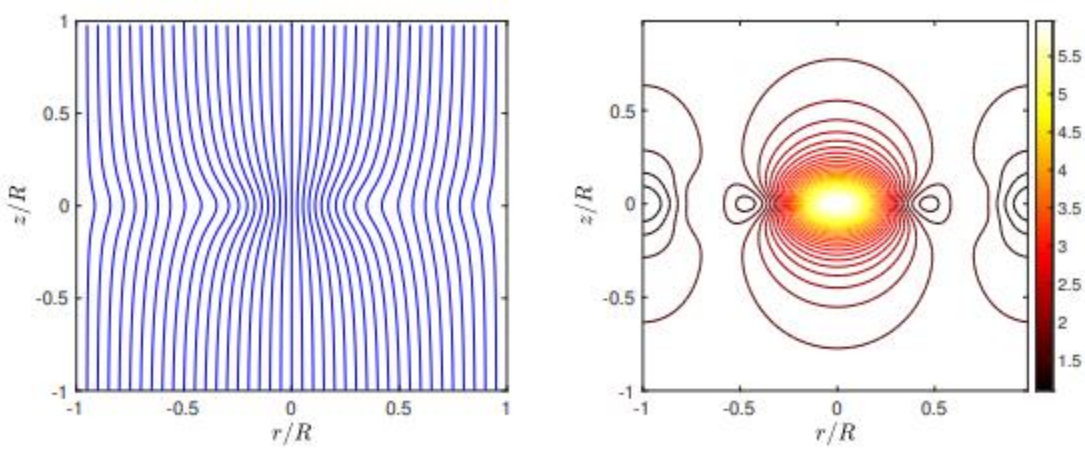

Figure 6: Background field $B = 0.5B_0$. **Left:** Magnetic field lines. **Right:** Contours of the total field strength.

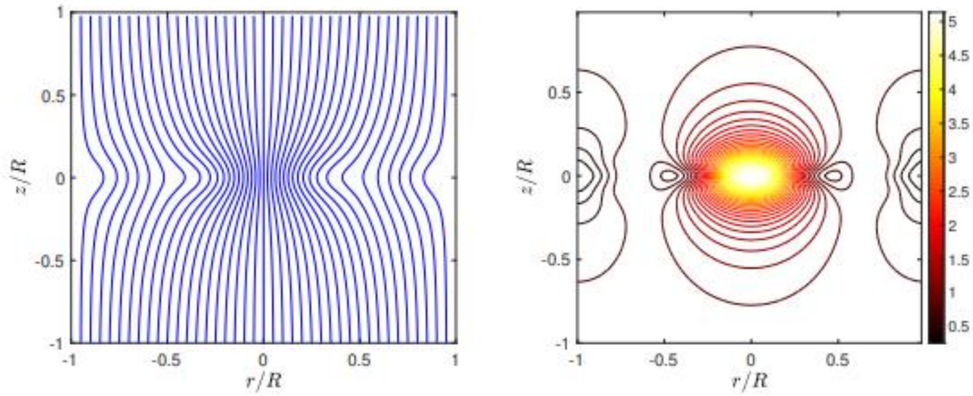

Figure 7: Background field $B = 0.25B_0$. **Left:** Magnetic field lines. **Right:** Contours of the total field strength.

This is normal, however the really intriguing property occurs as the field strength is diminished. The majority of the field strength is as yet concentrated at the core, however as B0 → 0 the hourglass 'squeeze' at the core is intensified.

The more vulnerable the outer field is, the more the field lines get contorted inside the core. This can give a sign by and by concerning how solid the general foundation field is concerning the field strength inside the core. Normally it would seem OK to make a fit to a model that is standardized to the foundation field.

Since the foundation field is a troublesome amount to quantify directly, one can reformulate 6.4 and 6.5 to being standardized to B0 which would yield solutions for Br and Bz standardized to the foundation field. This wouldn't transform anything as far as fitting polarization data since polarization maps just give data for Br/Bz thus a standardized model on a basic level actually can be utilized to fit polarization data.

Conclusion

Stars have for some time been known to be a significant factor in the development of the universe all in all, remembering for its constituent parts like worlds and planets. In this article, the formation of stars is considered in various developmental ages from the prestellar stage up to and including the formation and advancement of protostars.

A basic part in star formation is the magnetic field. A huge piece of this theory intends to study the magnetic field that administers both prestellar and protostellar cores. Involving hypothetical simulations related to observational data, vigorous models are fostered that give knowledge to a few significant heavenly properties administering the cores.

References

[1] Michaël Gillon. A novel seti strategy targeting the solar focal regions of the most nearby stars. Acta Astronautica, 94(2):629–633, 2014.

[2] Mark R Krumholz, Blakesley Burkhart, John C Forbes, and Roland M Crocker. A unified model for galactic discs: star formation, turbulence driving, and mass transport. Monthly Notices of the Royal Astronomical Society, 477(2):2716–2740, 2018.

[3] Frank H Shu, Fred C Adams, and Susana Lizano. Star formation in molecular clouds: observation and theory. Annual review of astronomy and astrophysics, 25(1):23–81, 1987.

[4] Ryo Kandori, Motohide Tamura, Nobuhiko Kusakabe, Yasushi Nakajima, Jungmi Kwon, Takahiro Nagayama, Tetsuya Nagata, Kohji Tomisaka, and Ken‚Äôichi Tatematsu. Distortion of magnetic fields in a starless core: Near-infrared polarimetry of fest 1–457. The Astrophysical Journal, 845(1):32, 2017.

[5] Telemachos Ch Mouschovias and Glenn E Ciolek. Magnetic fields and star formation: a theory reaching adulthood. pages 305–340, 1999.

[6] Mark R Krumholz and Christoph Federrath. The role of magnetic fields in setting the star formation rate and the initial mass function. Frontiers in Astronomy and Space Sciences, 6:7, 2019.

[7] Nigel R Minchin, Vitor HR Bonifacio, and Alexander G Murray. Submillimetre polarimetric observations of s140 and gl 2591: investigating the role of viewing angle on observed polarization position angles. Astronomy and Astrophysics, 315:L5–L8, 1996.

[8] Jacques P Vallée, Pierre Bastien, and Jane S Greaves. Highly polarized thermal dust emission in the bok globule cb 068. The Astrophysical Journal, 542(1):352, 2000.

[9] Edwin A Bergin and Mario Tafalla. Cold dark clouds: the initial conditions for star formation. Annu. Rev. Astron. Astrophys., 45:339–396, 2007.

[10] Tomoaki Matsumoto, Masahiro N Machida, Kohji Tomisaka, and Tomoyuki Hanawa. Self-gravitational collapse of a magnetized cloud core: high resolution simulations with three-dimensional mhd nested grid. Computer physics communications, 164(1-3):229–236, 2004.

[11] Masahiro N Machida, Shu-ichiro Inutsuka, and Tomoaki Matsumoto. Magnetic fields and rotations of protostars. The Astrophysical Journal, 670(2):1198, 2007.

[12] Takenori Nakano, Ryoichi Nishi, and Toyoharu Umebayashi. Mechanism of magnetic flux loss in molecular clouds. The Astrophysical Journal, 573(1):199, 2002.

[13] Bartek Ewertowski and Shantanu Basu. A mathematical model for an hourglass magnetic field. The Astrophysical Journal, 767(1):33, 2013.